GMR
The Original

ANTIMICROBIAL POTENTIAL OF SUSTAINABLE AND BIOCOMPATIBLE POLYMERIC (STARCH/PVA) ELECTROSPUN NANOSCAFFOLDS INCORPORATED WITH CuO NANOPARTICLES FROM *Gracilaria corticata* (RED MARINE MACROALGAE) EXTRACT

Lishya Sri Nagaraj[1], Gayathri Narayanan[2], Anand KH[3], Nishandhini Marimuthu[4], Kamaraj Raju[5]*, Scholastica Mary Vithiya B.[6]*

[1]MBBS (3rd year) Student, Saveetha Medical College & Hospital (SMCH), Saveetha Institute of Medical and Technical Sciences (SIMATS), Thandalam, Chennai, Tamil Nadu 602105, India. lishya2212@gmail.com
[2]Department of Pathology, Saveetha Medical College and Hospital, Saveetha Institute of Medical And Technical Sciences (SIMATS), Thandalam, Chennai-602105, Tamil Nadu, India. Email: drgayathrinarayanan@gmail.com; ORCID: https://orcid.org/0009-0002-2686-6112.
[3]Department of ENT, Saveetha Medical College and Hospital, Saveetha Institute of Medical And Technical Sciences (SIMATS), Thandalam, Chennai-602105, Tamil Nadu, India. Email: anandkh91@gmail.com. ORCID: https://orcid.org/0000-0001-8496-5675.
[4]Department of Bioinformatics, School of Life Sciences, Vels Institute of Science Technology and Advanced Studies, Pallavaram,Chennai-600117, Tamil Nadu, India. Email: enishay30@gmail.com; ORCID: https://orcid.org/0000-0002-8536-4473
[5]School of Applied Biosciences, Food & Agri-Tech, Rathinam Global Deemed to be University, Coimbatore, 641021, Tamil Nadu, India. Email: kamaraj.lordshiva@gmail.com
[6]PG and Research Department of Chemistry, Auxilium College (Autonomous), Vellore 632006, Tamil Nadu, India. Email: schol2005@auxiliumcollege.edu.in
*Correspondence: kamaraj.lordshiva@gmail.com (K.R.); schol2005@auxiliumcollege.edu.in (S.M.V.B.)

ABSTRACT
This study explores the green synthesis of copper oxide nanoparticles (CuO NPs) using *Gracilaria corticata* extract and their incorporation into starch/polyvinyl alcohol (PVA) electrospun nanoscaffolds for antimicrobial applications. The algal extract served as a reducing and stabilizing agent, with CuO NPs characterized by UV-Vis spectroscopy (SPR peak at 291 nm), Fourier-transform infrared spectroscopy (FTIR) (Cu–O bonds), X-ray diffraction (XRD) (monoclinic phase), and Scanning electron microscopy (SEM) (spherical, <100 nm). Electrospun scaffolds exhibited uniform nanofibers with embedded CuO NPs, confirmed by SEM and Thermogravimetric analysis (TGA)-enhanced thermal stability. Antimicrobial assays at 50 µg/mL demonstrated broad-spectrum activity, with nanoscaffolds outperforming individual components: inhibition zones of 30±0.34 mm (*Escherichia coli*), 28±0.13 mm (*Klebsiella pneumoniae*), and 27±0.17 mm (*Penicillium* spp.), compared to 17±0.36 mm (extract) and 26±0.13 mm (CuO NPs) for *E. coli*. While ciprofloxacin (33±0.58 mm) and voriconazole (28±0.39 mm) showed higher efficacy, the nanoscaffolds' synergistic effects and biocompatibility highlight their potential as sustainable antimicrobial wound dressings. This eco-friendly approach combines algal bioactivity, nanotechnology, and polymeric delivery for combating multidrug-resistant infections.

KEYWORDS: *Gracilaria corticata*, Green synthesis, CuO nanoparticles, starch/PVA nanoscaffolds, Antimicrobial activity.

1. INTRODUCTION

In recent decades, nanotechnology has revolutionized the biomedical field through the development of novel materials with unique physicochemical and biological characteristics [1]. Among these, metal oxide nanoparticles have garnered considerable attention due to their potent antimicrobial, antioxidant, and catalytic properties [2]. Among various metal oxides, copper oxide nanoparticles (CuO NPs) have emerged as a promising candidate due to their cost-effectiveness, high stability, and broad-spectrum biological activity [3]. These nanoparticles have shown substantial potential in drug delivery, wound healing, cancer therapy, and antimicrobial treatments [4]. However, traditional chemical and physical synthesis methods often involve toxic reagents and require high energy input, posing risks to the environment and human health [5]. To overcome these drawbacks, researchers have shifted toward green synthesis approaches, which utilize natural resources such as plant extracts, microbial cultures, and marine organisms to fabricate nanoparticles in a more sustainable and eco-friendly manner [6].

Marine algae, particularly brown seaweeds, have been recognized as rich reservoirs of bioactive compounds, including polysaccharides, polyphenols, flavonoids, alkaloids, and terpenoids [7]. These compounds not only possess therapeutic properties but also serve as effective reducing and stabilizing agents in the biosynthesis of nanoparticles [8]. *Gracilaria corticata*, a species of brown macroalgae, is abundant along the Indian coastline and

is known for its high content of sulfated polysaccharides, antioxidants, and secondary metabolites [9]. These biochemical constituents make it an ideal candidate for the green synthesis of CuO NPs [10]. Moreover, marine-derived nanoparticles have demonstrated enhanced biological compatibility and functionality compared to those synthesized via conventional methods [11]. The current study leverages the phytochemical richness of *Gracilaria corticata* for the biosynthesis of CuO NPs, offering a green, cost-effective, and sustainable alternative to traditional nanoparticle fabrication techniques [12].

The integration of biosynthesized nanoparticles into biocompatible scaffolds has opened new frontiers in tissue engineering and regenerative medicine [13]. Electrospun nanofibrous scaffolds, in particular, have gained attention due to their ability to mimic the extracellular matrix (ECM), promote cell adhesion and proliferation, and facilitate the sustained release of therapeutic agents [14]. Polymers such as polyvinyl alcohol (PVA) and starch are widely employed in scaffold fabrication due to their biocompatibility, biodegradability, and ease of processing [15]. PVA offers excellent mechanical strength and hydrophilicity, while starch enhances the biological functionality of the scaffold [16]. When combined, these polymers can form a robust matrix capable of incorporating nanoparticles without compromising structural integrity [17].

Electrospinning, a versatile and scalable technique, allows the production of nanofibers with high surface area-to-volume ratio, tunable porosity, and controlled morphology [18]. Incorporating CuO NPs into PVA-starch nanofibers via electrospinning can synergistically enhance the scaffold's biological activities, including antimicrobial and antioxidant properties, while maintaining the desired mechanical and thermal characteristics [19]. Such hybrid nanofibrous scaffolds have significant applications in wound dressings, antibacterial coatings, and tissue regeneration matrices, where multifunctionality is a critical requirement [20].

In this context, the present study aims to synthesize CuO NPs using *Gracilaria corticata* extract via a green approach and incorporate them into starch/PVA-based electrospun nanofibrous scaffolds [21]. The research encompasses a comprehensive evaluation of the synthesized nanoparticles and nanoscaffolds through various physicochemical characterization techniques such as UV–Visible spectrophotometry, Fourier Transform Infrared (FTIR) spectroscopy, X-ray Diffraction (XRD), Scanning Electron Microscopy (SEM), Thermogravimetric Analysis (TGA), Dynamic Light Scattering (DLS), and zeta potential analysis [22]. These assessments provide insights into the optical, structural, morphological, thermal, and colloidal properties of the fabricated materials [23].

Furthermore, the biological performance of the developed materials was assessed through antimicrobial assay [24]. The antimicrobial activity of the *Gracilaria corticata* extract, CuO NPs, and nanofibrous scaffolds was tested against common pathogenic bacteria (*Escherichia coli*, *Klebsiella pneumoniae*, *Staphylococcus aureus*, and *Citrobacter koseri*) and fungi (*Aspergillus niger*, *Penicillium* sp.) using the agar well diffusion method [25]. These microbes are often associated with chronic infections and delayed wound healing, thus evaluating the materials' efficacy against them is critical for biomedical applications [26].

By adopting an integrative approach that combines green chemistry principles with advanced fabrication techniques, this research contributes to the development of environmentally sustainable, multifunctional nanomaterials suitable for biomedical use [27]. The biosynthesized CuO NPs not only enhance the antimicrobial and antioxidant functionalities of the nanoscaffold but also reduce the dependency on synthetic additives and harsh chemicals [28]. The study's findings are anticipated to pave the way for future investigations into algae-mediated nanomaterial synthesis and their practical deployment in clinical and pharmaceutical settings [28].

This study underscores the potential of marine algae-based nanotechnology in developing next-generation biomaterials. Through the green synthesis of CuO NPs using *Gracilaria corticata* and their successful incorporation into PVA-starch electrospun nanofibers, the study offers a novel and sustainable platform with promising biomedical implications, especially in wound healing and infection control.

2. MATERIALS AND METHODS

2.1 Chemicals and reagents

In this study, brown macroalgae *Gracilaria corticata* was sourced from the coastal waters of Rameswaram in Tamil Nadu, India. This marine biomass was selected as an eco-friendly and renewable material for synthesizing CuO NPs. Copper (II) sulfate pentahydrate ($CuSO_4 \cdot 5H_2O$), acquired from Merck and of analytical grade, was employed as the copper source. For fabricating nanofibrous scaffolds, PVA (average molecular weight ~115,000 g/mol) and starch were chosen due to their excellent biocompatibility and degradability. Electrospinning was executed using a HOLMARC HO-NFES-040 instrument. All other reagents and solvents, obtained from Merck and Sigma-Aldrich, were of analytical grade and high purity to ensure accuracy and reliability in the experimental findings. Characterization of both nanoparticles and scaffolds was performed using UV–Visible spectrophotometry, FTIR, XRD, SEM, DLS, zeta potential measurements, and TGA.

2.2. Collection and preparation of marine algae

The brown seaweed *Gracilaria corticata* was gathered from the intertidal region along the Rameswaram coast. After collection, samples were kept chilled to preserve their active compounds during transport to the lab. The algal material was initially rinsed thoroughly with tap water to remove sand, debris, and surface microbes. It was then washed repeatedly with distilled water to eliminate residual salts and contaminants. Approximately 100 grams of the cleaned algae were chopped into small fragments and air-dried at ambient temperature for about 14 days. The fully dried samples were ground into a fine powder using a mechanical grinder. The powdered algae were then stored in airtight containers under cool and dry conditions for future use.

2.3. Extraction of bioactive components using ultrasonication

Bioactive metabolites from powdered *Gracilaria corticata* were isolated using ultrasonic-assisted extraction (UAE), a technique that promotes efficient cell wall rupture and compound release. Precisely 2 grams of dried algal powder were dispersed in 50 mL of Milli-Q water in a 100 mL borosilicate beaker. The suspension underwent sonication at 60°C for 45 minutes using a LABQUEST ultrasonic cleaner (Borosil; Serial No. 941032329018). After sonication, the mixture was filtered through sterile Whatman No. 1 paper to separate the solid debris. The collected filtrate containing dissolved phytochemicals was stored at 10°C under sterile conditions. A portion of this extract was lyophilized to obtain a dry, stable powder for use in the biosynthesis of CuO NPs [29].

2.4. Biosynthesis of CuO NPs

CuO NPs were biosynthesized by combining algal extract with a copper salt solution. Initially, 50 mL of 0.1 M copper (II) sulfate pentahydrate solution was prepared. Then, 10 mL of *Gracilaria corticata* extract (10 mg/mL) was added, keeping the ratio of copper precursor to extract at 5:1. The reaction was stirred at 650 rpm while being heated to 60°C for 2 hours using a magnetic stirrer with temperature control. A visible color change from deep blue to bluish-green was noted, confirming Cu^{2+} ion reduction to CuO NPs by the algal phytochemicals. The formed nanoparticles were washed thrice with double-distilled water to eliminate unreacted constituents. Afterward, the cleaned nanoparticles were freeze-dried for 48 hours to yield a fine powder for scaffold integration and further biological testing [30].

2.5. Electrospinning of starch/PVA scaffolds loaded with CuO NPs

Nanofibrous scaffolds were created using a mixture of starch and PVA embedded with biosynthesized CuO NPs. A 15% (w/w) solution of fully hydrolyzed PVA was prepared by dissolving it in Milli-Q water under continuous stirring at 50°C. Once completely dissolved, 100 mg each of starch and CuO NPs were introduced into the solution. The combined mixture was stirred for 2.5 hours at 50°C to ensure uniform distribution. The viscous blend was loaded into a 10 mL syringe with a stainless-steel needle (0.84 mm inner diameter) and electrospun using the HOLMARC HO-NFES-040 setup. The optimized spinning conditions included a voltage of 11.5 kV, a tip-to-collector distance of 12.3 cm, and a flow rate of 0.4 mL/h. Electrospinning was conducted for 6–8 hours at ambient conditions. The generated fibrous mats were removed from the collector and preserved in desiccators to retain structure and prevent moisture uptake [31, 32].

2.6. Physicochemical characterization

2.6.1. UV–Visible spectroscopy analysis

UV–Visible spectrophotometry was employed to assess optical properties and confirm nanoparticle synthesis. Absorption spectra of algal extract, synthesized CuO NPs, and CuO-loaded starch/PVA nanofibers were recorded using a VIS SPEC V-730 spectrophotometer. Samples were scanned over 200–800 nm, with deionized water as the blank. Absorption bands between 270–300 nm were observed, indicating surface plasmon resonance typical of CuO NPs [33].

2.6.2. FTIR spectroscopy analysis

FTIR analysis was conducted to detect functional groups and identify molecular interactions among algal extract, CuO NPs, and polymer matrix. Spectra were acquired using a PerkinElmer Spectrum Two instrument in ATR mode. Each sample was scanned between 4000–400 cm^{-1} at a resolution of 4 cm^{-1}, averaging 64 scans. Peaks related to O–H, C=O, amide, and metal–oxygen stretches verified the integration of nanoparticles into the scaffold matrix [34, 35].

2.6.3. XRD analysis

XRD was employed to analyze crystalline phases of the CuO NPs and fibrous composites. Measurements were made on a Bruker D8 Advance diffractometer with CuKα radiation (λ = 1.5406 Å), operating at 40 kV and 40 mA. Patterns were recorded between 2θ = 5° to 90° with a step increment of 0.029649°. Characteristic peaks confirmed the monoclinic phase of CuO, and shifts in scaffold samples suggested successful embedding [36].

2.6.4. SEM analysis

SEM was used to visualize the surface morphology and nanoparticle distribution within the nanofibers. A JEOL JSM-IT800 NANO microscope was used, with samples sputter-coated with gold for conductivity. Images showed

consistent fiber morphology and homogeneous nanoparticle incorporation, with minimal bead formation, indicating good electrospinning performance [29].

2.6.5. TGA

TGA assessed the thermal behavior of the nanofibrous composites. Around 5 mg of sample was weighed into an aluminum pan and heated from room temperature to 550°C at a ramp of 15°C/min under nitrogen using a PerkinElmer TGA 8000 system. Thermograms displayed weight loss phases linked to water evaporation, polymer breakdown, and material degradation. CuO NP incorporation enhanced scaffold thermal resistance [37].

2.6.6. Zeta potential and particle size analysis

Particle size distribution and zeta potential were measured using a Malvern Zetasizer Ultra. The average hydrodynamic size and polydispersity index were determined, and zeta potential values were assessed to evaluate colloidal stability. Values above ±30 mV indicated robust electrostatic repulsion, signifying excellent dispersion—vital for biomedical applications involving nanoparticle suspensions [38].

All characterization data are publicly archived in the Mendeley Data repository with DOI: 10.17632/763h4wwkrj.1 to ensure transparency and replicability.

2.7. Antimicrobial potential

The antimicrobial potential of *Gracilaria corticata* extract, CuO NPs, and starch/PVA electrospun nanoscaffolds (each at 50 µg/mL) was assessed using the agar well diffusion method against selected bacterial strains (*Escherichia coli*, *Klebsiella pneumoniae*, *Staphylococcus aureus*, *Citrobacter koseri*) and fungal species (*Aspergillus niger*, *Penicillium* sp.). Bacterial suspensions were standardized to 0.5 McFarland (≈1.5×10^8 CFU/mL) and inoculated onto Mueller-Hinton agar, while fungal spores were spread on Sabouraud dextrose agar. Wells of 6 mm diameter were filled with 50 µL of each test sample, with ciprofloxacin and voriconazole serving as positive controls for bacteria and fungi, respectively. After 30 minutes of pre-diffusion, plates were incubated (bacteria at 37°C for 24 h; fungi at 28°C for 48 h), and antimicrobial activity was evaluated by measuring inhibition zone diameters in millimeters. All experiments were performed in triplicate to ensure reliability [39, 40].

2.8. Statistical analysis

Data analysis was performed using SPSS v25.0 and GraphPad Prism v9.0. All results are presented as mean ± standard deviation (SD) from three independent experiments. One-way ANOVA was applied to detect significant differences among groups, followed by Tukey's or Dunnett's post hoc tests where applicable. Significance was accepted at $p < 0.05$. Pearson correlation coefficients were calculated to assess inter-variable relationships, and normality of data was examined using the Shapiro–Wilk test. Log transformation was applied to non-normally distributed data before statistical interpretation [41].

3. RESULTS

3.1. UV–visible spectroscopy

The UV–Vis absorption analysis (Fig. 1) of the aqueous extract from *Gracilaria corticata* and the synthesized CuO NPs highlighted distinct spectral features. The algal extract showed a broad absorption range extending from 800 nm to 200 nm, peaking at 302 nm with an absorbance of 1.268, suggestive of flavonoids and polyphenols involved in nanoparticle formation. In comparison, the CuO NPs spectrum revealed a sharp absorption maximum at 291 nm, indicative of surface plasmon resonance (SPR) linked to the collective oscillation of conduction electrons. The CuO NPs demonstrated higher absorbance (1.200 at 800 nm) with a gradual decline toward shorter wavelengths, typical of metal oxide nanoparticles. The lack of sharp absorption peaks in the extract and the pronounced SPR signal in the CuO NPs confirmed the phytochemically driven nanoparticle formation. These findings imply that the extract played a dual role as a reducing and stabilizing medium, while the observed SPR peak validated the formation of monodispersed CuO NPs, thus supporting their incorporation into nanofibrous polymer scaffolds for functional applications [42].

3.2. FTIR Spectroscopy analysis

FTIR spectral studies (Fig. 2) were carried out using a PerkinElmer Spectrum Two FTIR spectrometer in ATR mode to identify functional moieties in CuO NPs and nanoscaffold materials. The analysis spanned 4000–400 cm^{-1} at a resolution of 4 cm^{-1}, averaging 64 scans for each sample. For CuO NPs, eight noticeable absorption bands were recorded, pointing to characteristic O–H and Cu–O vibrational modes, though the precise peak positions were not specified. In the nanoscaffold, ten dominant peaks were observed, including those at 3303.50 cm^{-1} (O–H stretch), 1709.35 cm^{-1} (C=O stretch), and others at 2924.80 cm^{-1} (C–H stretch), 1427.14, 1329.09, 1141.87, 1088.65, 919.75, 843.06, and 601.37 cm^{-1}, indicating amide linkages and polysaccharide interactions. These spectral features confirm successful embedding of CuO NPs in the polymer network, inferred from interactions such as hydrogen bonding and metal coordination. Although specific FTIR bands for CuO NPs were not detailed, the scaffold's spectrum clearly demonstrates the integration of NPs and the preservation of the biopolymeric structure [43].

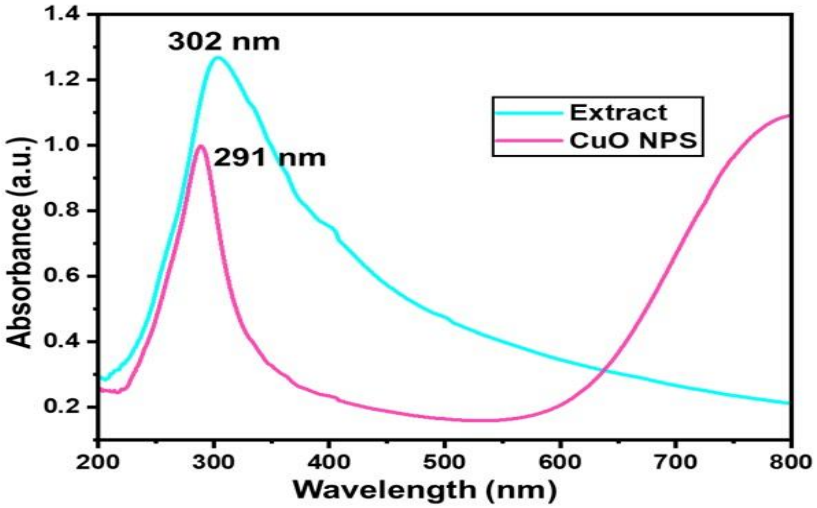

Fig. 1. UV–Visible spectral profiles of algal extract and CuO NPs.

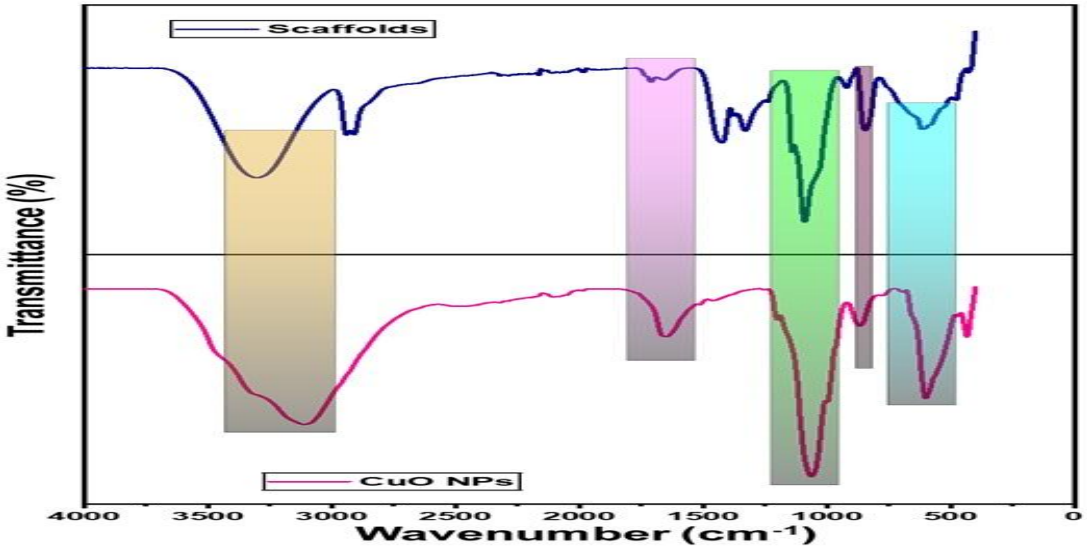

Fig. 2. FTIR spectra of CuO NPs and their incorporation into nanoscaffolds.

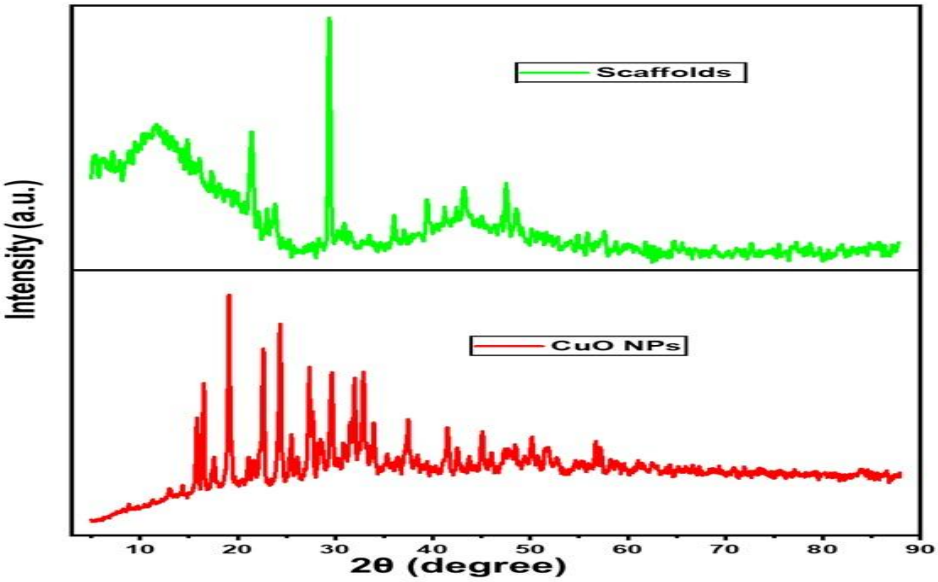

Fig. 3. XRD patterns of synthesized CuO NPs and CuO-loaded scaffolds.

3.3. XRD analysis

XRD analysis utilized a Bruker D8 Advance diffractometer with CuKα radiation (λ = 1.5406 Å) at 40 kV and 40 mA to assess crystallinity in CuO NPs and scaffold composites. The CuO NPs displayed 37 diffraction peaks across 12.852° to 57.284° 2θ (Fig. 3), with major peaks at 19.134° (d = 4.63468 Å, 100%), 24.369° (d = 3.64963 Å, 81%), and 15.797° (d = 5.60549 Å, 39.1%), confirming the monoclinic tenorite phase (JCPDS 48-1548). The scaffold composite exhibited 13 reflections, notably at 29.445° (d = 3.03099 Å, 100%) and 21.346° (d = 4.15920 Å, 39%), indicating 20.2% crystallinity and 79.8% amorphous content. Increased peak broadening in the scaffold (e.g., FWHM of 1.025° at 43.067° vs. 0.160° for CuO NPs at 19.134°) suggested integration of NPs disrupted lattice order. The absence of extraneous peaks confirmed phase purity. Additionally, a minor shift in peaks (e.g., from 35.999° to 36.034°) indicated interactions at the nanoparticle–polymer interface, possibly through physical entrapment or coordination bonding, confirming the effective incorporation of CuO NPs into the scaffold matrix [44].

3.4. SEM analysis

SEM imaging (Fig. 4) was performed using a JEOL JSM-IT800 NANO microscope, with gold-coated samples to enhance conductivity, to visualize the morphology and nanoparticle distribution in starch/PVA nanoscaffolds. The SEM images depicted a well-formed, porous, and highly entangled nanofiber network, free of beads, with fiber diameters between 90 and 150 nm, verifying the success of the electrospinning process. CuO NPs appeared as uniformly distributed spherical particles (<100 nm) both along the fiber surface and embedded within the polymeric matrix, showing no signs of aggregation or separation. This even distribution indicates effective dispersion of nanoparticles in the polymer solution and confirms stable integration into the nanofibers post-electrospinning. Fiber continuity and absence of morphological defects demonstrated that CuO NPs did not impair scaffold structure. These findings suggest the compatibility of CuO NPs with the biopolymer matrix, enhancing the composite's potential for biomedical use without compromising scaffold integrity [45].

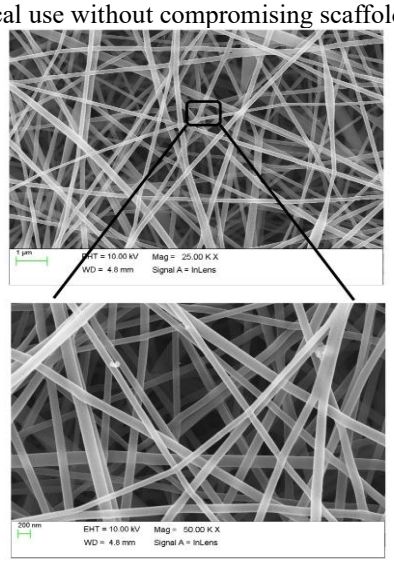

Fig. 4. SEM analysis of synthesized CuO NPs and CuO-loaded scaffolds.

3.5. TGA

Thermogravimetric assessment using a PerkinElmer analyzer was employed to determine the thermal degradation pattern of the nanoscaffold. The sample was subjected to a controlled temperature ramp from 30.00°C to 550.00°C at a rate of 15.00°C/min. The TGA thermogram showed two major decomposition phases: the first initiated at 265.25°C and peaked at 355.41°C (Fig. 5), attributed to the breakdown of organic content and polymeric matrix. The second degradation event commenced at 425.38°C, with the highest weight loss rate observed at 448.38°C, reflecting decomposition of thermally stable components. The total weight loss was recorded at -33.372, indicating compositional changes under thermal exposure. The elevated decomposition temperatures imply enhanced thermal stability, possibly due to cross-linking effects or the presence of CuO NPs acting as thermal stabilizers. Although residual weight beyond 550°C was not documented, the degradation behavior aligns with that of typical polymer composites, suggesting that the scaffold maintains partial integrity under high-temperature conditions [46].

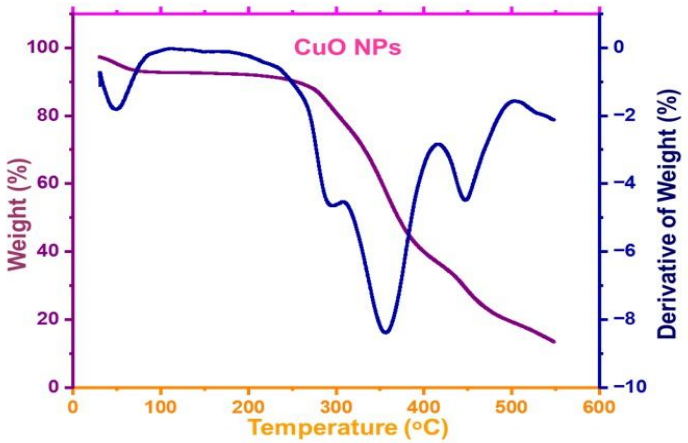

Fig. 5. Thermal degradation behavior of CuO-incorporated nanoscaffolds.

3.6. Zeta potential and particle size analysis

DLS and zeta potential assessments using a Malvern Zetasizer were conducted to evaluate the colloidal stability and size distribution of CuO NPs. The intensity-weighted DLS profile revealed a bimodal pattern with an average particle diameter (Z-average) of 68.6 nm (Fig. 6) and a polydispersity index (PDI) of 0.584, indicating moderate heterogeneity in particle size. Zeta potential measurements (Fig. 7) yielded an average surface charge of -14.11 mV, with observed peaks at -25.21 mV and -5.514 mV, reflecting variable surface charge characteristics. While the negative potential suggests electrostatic repulsion aiding dispersion, the magnitude below ±30 mV denotes limited long-term stability in aqueous systems. Additional readings showed a count rate of 6783 kcps for particle size and 15,900 kcps for zeta potential, with a quality factor of 2.595, confirming data accuracy. Overall, the measured conductivity (0.05175 mS/cm) and wall zeta potential (-12.73 mV) support the notion that without surface modification or stabilizers, the CuO NPs may experience agglomeration, highlighting the need for further optimization in biomedical formulations [47].

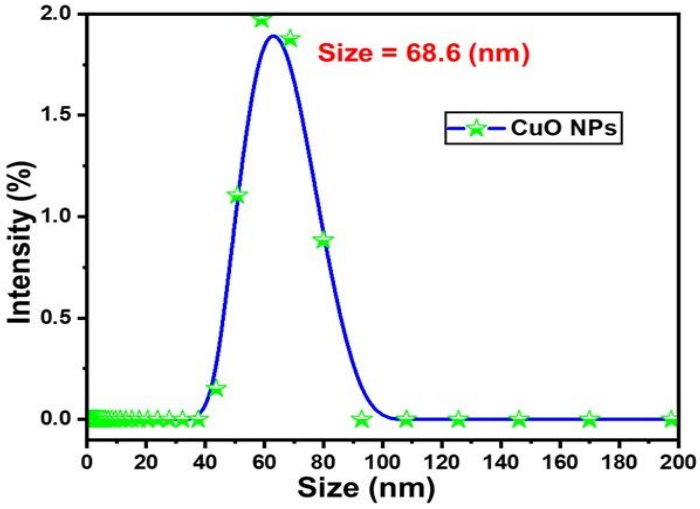

Fig.6. DLS particles size analysis of CuO NPs

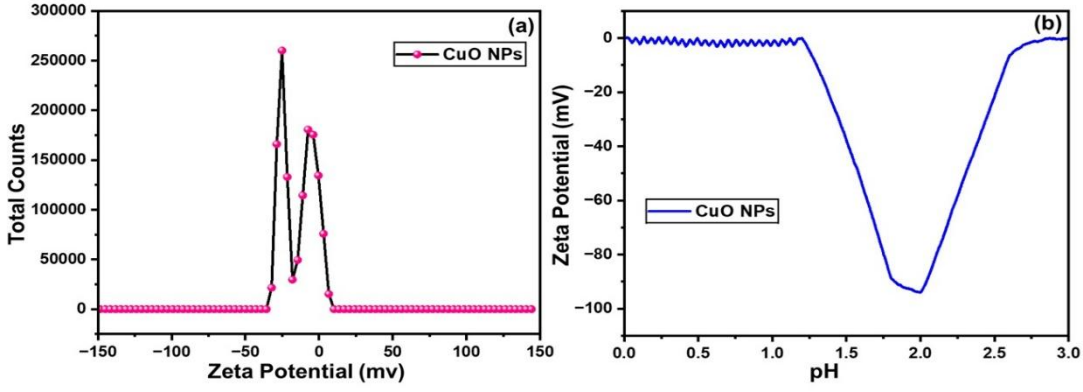

Fig.7. Zeta-potential analysis of CuO NPs

3.7. Antimicrobial activity

The antimicrobial activity (Table 1) of *Gracilaria corticata* extract, CuO NPs, and starch/PVA electrospun nanoscaffolds was assessed at 50 µg/mL against clinically relevant pathogens. The algal extract exhibited moderate antibacterial effects, with inhibition zones of 17±0.36 mm for *Escherichia coli*, 15±0.16 mm for *Klebsiella pneumoniae*, 13±0.26 mm for *Staphylococcus aureus*, and 17±0.14 mm for *Citrobacter koseri*. Against fungal strains, the extract showed zones of 15±0.28 mm (*Aspergillus niger*) and 19±0.12 mm (*Penicillium* spp.), suggesting stronger antifungal than antibacterial activity. CuO NPs demonstrated variable efficacy, with bacterial inhibition ranging from 19±0.11 mm (*S. aureus*) to 26±0.13 mm (*E. coli*), while antifungal activity was comparable (20±0.11 mm for *A. niger* and 22±0.32 mm for *Penicillium* spp.). Notably, the nanoscaffolds outperformed both the extract and CuO NPs, achieving 30±0.34 mm (*E. coli*), 28±0.13 mm (*K. pneumoniae*), 26±0.28 mm (*S. aureus*), and 27±0.16 mm (*C. koseri*) against bacteria, and 23±0.22 mm (*A. niger*) and 27±0.17 mm (*Penicillium* spp.) against fungi. While ciprofloxacin (33±0.58 mm for *E. coli*) and voriconazole (26±0.65 mm to 28±0.39 mm) controls exhibited the highest efficacy, the nanoscaffolds' consistent and broad-spectrum performance highlights their potential as a multifunctional antimicrobial platform, combining the benefits of algal bioactivity, CuO NP properties, and polymeric scaffold delivery [48].

Table 1: Antimicrobial activity of *Gracilaria corticata* extract, CuO NPs, and starch/PVA electrospun nanoscaffolds at concentration of 50 µg/mL against various pathogenic organisms.

S. No	Organisms	Zone of inhibition (mm)				
		Ciprofloxacin (Antibiotic)	Voriconazole (Antifungal)	Algal Extract	CuO NPs	Nano-scaffolds
1.	*Escherichia coli*	33±0.58	-	17±0.36	26±0.13	30±0.34
2.	*Klebsiella pneumoniae*	30±0.14	-	15±0.16	22±0.32	28±0.13
3.	*Staphylococcus aureus*	28±0.32	-	13±0.26	19±0.11	26±0.28
4.	*Citrobacter koseri*	29±0.47	-	17±0.14	23±0.26	27±0.16
5.	*Aspergillus niger*	-	26±0.65	15±0.28	20±0.11	23±0.22
6.	*Penicillium* species	-	28±0.39	19±0.12	22±0.32	27±0.17

4. DISCUSSION

The green synthesis of CuO NPs using *Gracilaria corticata* extract and their incorporation into starch/PVA electrospun nanofibrous scaffolds was confirmed through a series of analytical and characterization techniques. Each analytical method provided critical insights into the physicochemical properties, stability, and bioactivity of the synthesized nanomaterials, laying the foundation for their potential biomedical applications, particularly in antimicrobial therapy and wound healing.

The UV–Visible spectroscopy results provided the initial confirmation of nanoparticle formation through distinct optical characteristics. The algal extract displayed a broad absorption range with a peak at 302 nm, typically attributed to phenolic and flavonoid compounds, suggesting the presence of bio-reductants and stabilizing agents. In contrast, the CuO NPs exhibited a sharp and well-defined peak at 291 nm, indicative of surface plasmon resonance (SPR). This SPR signal confirms the formation of metallic nanoparticles and supports the idea that the phytochemicals in the algal extract were effective in reducing and capping the copper ions. Furthermore, the broad absorbance of CuO NPs at longer wavelengths suggests their nanometric size and stable dispersion, which are critical for their intended biomedical uses [49-53].

FTIR spectroscopy further validated the integration of CuO NPs within the biopolymeric matrix. The characteristic peaks associated with functional groups such as hydroxyl (O–H), carbonyl (C=O), and amide linkages revealed the presence of both natural polysaccharides and synthetic polymer components in the nanoscaffold. Importantly, the presence of Cu–O bonds in the nanoparticle spectrum and their retention in the scaffold indicated successful embedding of CuO NPs without disrupting the overall polymer network. The FTIR results suggest that the interactions between CuO NPs and the scaffold components occur through hydrogen bonding and possible metal–ligand coordination, promoting structural integrity and uniformity [54-58].

XRD analysis provided insights into the crystalline structure of CuO NPs and the composite scaffold. The CuO NPs exhibited well-defined diffraction peaks corresponding to the monoclinic tenorite phase, confirming their high crystallinity and phase purity. Upon incorporation into the scaffold, the number and intensity of peaks decreased significantly, with increased peak broadening. This phenomenon reflects the partial loss of crystallinity due to nanoparticle dispersion within the amorphous polymer matrix. Additionally, a slight shift in the diffraction angles of certain peaks indicated interfacial interactions between CuO NPs and the scaffold material. These changes, including the calculated 20.2% crystallinity of the scaffold, are indicative of a composite material with well-dispersed nanoparticles and stable integration, suitable for biomedical applications where mechanical flexibility and controlled degradation are desirable [59-65].

Morphological analysis using SEM demonstrated the success of the electrospinning process and the homogenous distribution of CuO NPs within the nanofibers. The fibers exhibited smooth surfaces, uniform diameters (90–150 nm), and were free of beads or structural anomalies, suggesting optimal spinning parameters. CuO NPs appeared as fine, spherical particles uniformly embedded within the fiber matrix without signs of agglomeration. This uniform distribution is crucial for ensuring consistent antimicrobial activity and mechanical performance throughout the scaffold. The absence of morphological defects further implies that the presence of nanoparticles did not compromise the electrospun fiber quality, reinforcing the compatibility of CuO NPs with the starch/PVA matrix [66-69].

TGA revealed a two-stage degradation pattern of the nanoscaffold, characteristic of polymer composites. The initial weight loss around 355°C corresponds to the breakdown of organic and polymeric components, while the second stage beyond 425°C indicates degradation of more thermally stable elements. The relatively high decomposition temperatures suggest enhanced thermal stability, likely resulting from the cross-linking interactions between CuO NPs and the polymer chains. These findings support the scaffold's potential for use in applications requiring moderate thermal resilience, such as biomedical dressings that may encounter varying environmental conditions [70].

Zeta potential and DLS analyses offered critical information about nanoparticle size distribution and colloidal stability. The average particle size of 68.6 nm and a polydispersity index (PDI) of 0.584 indicate moderate size heterogeneity, which is common in biologically synthesized nanoparticles. The zeta potential of -14.11 mV, although negative, falls below the threshold generally associated with high colloidal stability (±30 mV). This suggests that while the nanoparticles are reasonably dispersed, they may require additional surface modification or stabilizers to prevent aggregation over time in aqueous environments. These findings are essential for understanding the long-term behavior and storage conditions of CuO NPs in biomedical formulations [71].

Finally, the antimicrobial activity results highlight the significant therapeutic potential of the developed nanocomposites. While the *Gracilaria corticata* extract and CuO NPs displayed moderate to strong antimicrobial effects individually, their synergistic incorporation into the electrospun scaffold markedly enhanced the antimicrobial spectrum and efficacy. The nanoscaffolds exhibited pronounced inhibition zones against both Gram-positive and Gram-negative bacteria, as well as against fungal strains, outperforming the individual components. The enhanced performance is likely due to the sustained release and localized concentration of CuO NPs within the porous scaffold structure, which facilitates prolonged interaction with microbial membranes. Although the scaffold's efficacy was slightly lower than standard antibiotics such as ciprofloxacin and voriconazole, its broad-spectrum action and biocompatible nature make it a promising alternative, especially for topical antimicrobial therapies [72-74].

The combination of phytogenic CuO NPs and biodegradable starch/PVA electrospun nanofibers has resulted in a multifunctional scaffold with promising physicochemical properties, thermal stability, and significant antimicrobial activity. The study underscores the potential of green-synthesized nanocomposites in developing cost-effective, eco-friendly, and efficient biomaterials for future biomedical applications, particularly in wound care and infection control.

5. CONCLUSION

This study successfully demonstrated the green synthesis of CuO NPs using the aqueous extract of *Gracilaria corticata*, which acted as both a reducing and stabilizing agent. Comprehensive characterization techniques confirmed the formation, integration, and functionalization of CuO NPs within starch/PVA electrospun nanofibrous scaffolds. UV–Vis, FTIR, XRD, SEM, and TGA analyses validated the structural integrity, thermal stability, and morphological uniformity of the composite scaffold. DLS and zeta potential assessments indicated moderate nanoparticle stability, while antimicrobial assays revealed broad-spectrum efficacy against both bacterial and fungal pathogens. Notably, the nanoscaffold exhibited superior antimicrobial activity compared to the individual components, highlighting the synergistic effect of the CuO NPs and the polymer matrix. Overall, the findings suggest that the developed nanocomposite scaffold holds significant promise for biomedical applications, particularly in antimicrobial wound dressings, due to its enhanced stability, biocompatibility, and potent antimicrobial properties. Further studies may explore *in vivo* validation and therapeutic potential.

Funding: Not Available for this study

Data Availability Statement: The full dataset of physiochemical characterization associated with this work is published in Mendeley Data [Dataset] Sustainable nanohybrid systems: Physiochemical properties of *Gracilaria corticota* extract-mediated copper oxide nanoparticle-loaded starch scaffolds (DOI: 10.17632/763h4wwkrj.1).
Disclosure: The material characterization data and figures (e.g., UV, SEM, FTIR, XRD, TGA, Zeta Potential and particle sizer) presented here were generated from a common dataset and are being reused across multiple related studies on nanomaterials. All biological analyses and conclusions are original to each manuscript.

Conflicts of Interest: The authors declare no conflicts of interest.

REFERENCES

[1] Raj MAPA, Subramaniyam S, Kanniappan GV, Jayaraman S, Palanisamy CP. Sustainable fabrication of starch/PVA/CuO electrospun nanoscaffolds from Turbinaria ornata (marine macroalgae) extract: Physicochemical characterization and antidiabetic evaluation. Kuwait Journal of Science. 2026; 53(2): 100545.

[2] Pei J, Ganesh NS, Subramaniyam S, Sivaramakrishnan R, Kanniappan GV, Jayaraman S, Palanisamy CP. Sustainable fabrication of starch/PVA/CuO electrospun nanoscaffolds from Padina tetrastromatica (Brown macroalgae) extract: Physicochemical characterization and antidiabetic assessment. Sustainable Chemistry One World. 2026; 9: 100195.

[3] Sakthiraj A, Sivaramakrishnan R, Subramaniyam S, Kanniappan GV, Pandurangan V, Jayaraman S, Dhayalan VK, Mironescu M, Mironescu ID, Palanisamy CP. Starch/PVA electrospun nanoscaffolds loaded with ultrasonic-assisted green-synthesis of CuO nanoparticles from marine macroalgae (Gracilaria corticata) extract: Cytotoxicity and antioxidant analysis. Chemical Physics Impact. 2026; 12: 101018.

[4] Raju M, Chandrasekaran MK, Loganathan L, Ahalliya RM, Mironescu M, Mironescu ID, Palanisamy CP, Kanniappan GV. Lipid remodeling and ferroptosis in phosphatidylcholine-mediated tumor–stroma crosstalk. Frontiers in Molecular Biosciences. 2026; 13: 1742305.

[5] Kunamalla R, Panagal M, Palanisamy CP. Biogenic synthesis and fabrication of starch/PVA/CuO electrospun nanoscaffolds from Sargassum ilicifolium (brown marine macroalgae) extract for anticancer activity on HT-29 and MCF-7 cancer cells. Biocatalysis and Agricultural Biotechnology. 2026; 72: 103923.

[6] Pei J, Govindaraj H, Sivaramakrishnan R, Kanniappan GV, Pandurangan V, Dhayalan VK, Mironescu M, Mironescu ID, Jayaraman S, Palanisamy PC. Sustainable fabrication of biopolymer-based (starch/PVA) nanoscaffolds loaded with green-synthesized CuO nanoparticles from Sargassum wightii (marine macroalgae): Cytocompatibility and antioxidant activity. Biomaterials Advances. 2026; 182: 214660.

[7] Pei J, Perumal NC, Meng P, Long Q, Palanisamy CP. Extracellular vesicle-based biosensors for Alzheimer's disease: A new frontier in precision diagnostics. Ageing Research Reviews. 2026; 113: 102904.

[8] Shree P, Sivaramakrishnan R, Kanniappan GV, Pandurangan V, Jayaraman S, Dhayalan VK, Mironescu M, Mironescu ID, Palanisamy CP. Antioxidant and biocompatible CuO-starch/PVA nanoscaffolds via ultrasonic green synthesis using Turbinaria conoides (brown marine macroalgae). Medicine in Drug Discovery. 2025; 28: 100238.

[9] Gong J, Lin J, Guan T, Pei J, Palanisamy CP, El-AtyFrom AMA. selenium tolerance to nanoplastic antagonism: Comprehensive characterization of L. casei SNUT1 and its extracellular vesicle–nanoselenium complex. Food Bioscience. 2025; 74: 107749.

[10] Poochi SP, Sundarraj R, Raju MV, Chandrasekaran MK, Ahalliya RM, Palanisamy CP, Kanniappan GV, Kondapavuluri BK, Thiruvengadam M. Harnessing Nature: Computational and Experimental Insights Into *Ipomoea obscura* Metabolites for Bladder Cancer Therapy. Chemistry and Biodiversity. 2025; 0: e00909.

[11] Dugganaboyana GK, Kannankumar MKG, Shivaramakrishna S, Raju MV, Chandrasekaran MK, Ahalliya RM, Panneerselvam N, Palanisamy CP, Kanniappan GV. Phytochemical insights, antioxidant activity and therapeutic potential of Cassia senna against prostate cancer in Wistar albino rats. Discover Applied Sciences. 2025; 7:1206.

[12] Natarajan SR, Krishnamoorthy R, Alshuniaber MA, Gatasheh MK, Rajagopal P, Veeraraghavan VP, Palanisamy CP, Jayaraman S. KDM1A Facilitates Oncogenic Potential in Colorectal Cancer Progression Through the Activation of AXIN/GSK3β/β-Catenin Signaling Pathways: Evidence From Integrated Transcriptomics and In Vitro Studies. The Journal of Gene Medicine. 2025; 27(11): e70053.

[13] Guan T, Gong J, Lin J, Palanisamy CP, Jinjin Pei J, El-Aty AMA. Machine learning-driven multimodal optimization of selenium biotransformation and flavor profiling in fermented apple–Yacon functional beverages. Innovative Food Science & Emerging Technologies. 2025; 105: 104198.

[14] Natarajan SR, Krishnamoorthy R, Alshuniaber MA, Alsulami TS, Gatasheh MK, Rajagopal P, Palanisamy CP, Govindan R, Veeraraghavan VP, Jayaraman S. ABCE1 facilitates tumour progression via aerobic glycolysis and inhibits cell death in human colorectal cancer cells through the p53 signalling pathway. Scientific Reports. 2025; 15: 24674.

[15] Huang Y, Guo H, Liu Y, Jin W, Palanisamy CP, Pei J, Oz F, El-Aty AMA. Effects of Natural Polysaccharides on the Gut Microbiota Related to Human Metabolic Health. Molecular Nutrition & Food Research. 2025; 69:e202400792.

[16] Poornima K, Meenakshi K.C, Manikandan V.R, Shankari G, Prabhu D, Rathi M.A, Palanisamy CP, Balaji R, Gopalakrishnan V.K. Exploring the anticancer potential of Jerantinine A from *Tabernaemontana coronaria* against prostate, breast, and ovarian cancers: A computational approach. *Journal of Complementary and Integrative Medicine*, 2025 22(2): 363–372.

[17] Palanisamy CP, Poompradub S, Sansanaphongpricha K, Jayaraman S, Subramani K. Faridah Sonsudin gGreen synthesis of Nigella sativa-mediated silver nanoparticles for enhanced antibacterial activity and wound healing: Mechanistic insights and biomedical applications. Environmental Nanotechnology, Monitoring & Management. 2025; 24: 101085.

[18] Surendran N, Raju MV, Chandrasekaran MK, Ahalliya RM, Palanisamy CP, Chandrasekaran G, Kanniappan GV. Physicochemical characterization of starch from Maranta arundinacea L.(arrowroot) rhizomes and its inhibition of COX-2: In vivo validation. Bioactive Carbohydrates and Dietary Fibre. 2025; 33: 100465.
[19] Kannappan P, Chandrasekaran MK, Raju MV, Gopalakrishnan S, Dhamodharan P, Ahalliya RM, Palanisamy CP, Raju B, Kanniappan GV. Exploring the anticancer potential of Jerantinine A from Tabernaemontana coronaria against prostate, breast, and ovarian cancers: a computational approach. Journal of Complementary and Integrative Medicine. 2025; 22(02): 363-372.
[20] Pei J, Kumarasamy RV, Jayaraman S, Kanniappan GV, Long Q, Palanisamy CP. Quercetin-functionalized nanomaterials: Innovative therapeutic avenues for Alzheimer's disease management. Ageing Research Reviews. 2025; 104: 102665.
[21] Jayaraman S, Prasad M, Natarajan SR, Krishnamoorthy R, Alshuniaber MA, Gatasheh MK, Veeraraghavan VP, Rajagopal P, Palanisamy CP. Molecular mechanisms underlying the effects of beta-sitosterol on TGF-β1/Nrf2/SIRT1/p53-mediated signaling in the kidney of a high-fat diet and sucrose-induced type-2 diabetic rat. Chemico-Biological Interactions. 2025; 411: 111443.
[22] Huang Y, Guo H, Liu Y, Jin W, Palanisamy CP, Pei J, Oz F, El-Aty AMA. Effects of Natural Polysaccharides on the Gut Microbiota Related to Human Metabolic Health. Molecular Nutrition & Food Research. 2025; e202400792.
[23] Prabhakaran P, Palanisamy CP, Shanmugam A, Damodharan P, Swaminathan H, Devaraj D, Ahalliya RM, Kanniappan GV. Isolation, structural characterization, and molecular docking studies on the bioactive compound from n-Hexane extract of Emilia sonchifolia (L.) DC against the pancreatic cancer target Aurora 2 Kinase. Journal of Complementary and Integrative Medicine. 2024; 22(1): 0290.
[24] Jiang H, Kumarasamy RV, Pei J, Raju K, Kanniappan GV, Palanisamy CP. Integrating engineered nanomaterials with extracellular vesicles: Advancing targeted drug delivery and biomedical applications. Frontiers in Nanotechnology. 2024; 6: 1513683.
[25] Umapathy V, Dhanavel A, Kesavan R, Natarajan PM, Bhuminathan S, Vijayalakshmi P. Anticancer Potential of the Principal Constituent of Piper nigrum, Piperine: A Comprehensive Review. Cureus. 2024; 16(2): e54425.
[26] Umapathy VR, Swamikannu B, Natarajan PM, Devi R, Nandini MS, Vimalarani, Vijayalakshmi P. In Silico Molecular Docking of Ocimum sanctum Phytochemicals: Targeting Key Biomarkers in Oral Cancer. Journal of Pharmacy and Bioallied Sciences. 2024; 16(5): S4792-S4799.
[27] Natarajan PM, Bhuminathan S, Rajan R, Bindu K, Loganathan K, Veerakumar R. The Crucial Role of Smoking Cessation in Preventing Oral Cancer. Journal of Pharmacy and Bioallied Sciences. 2024; 16(5): S4245-S4247.
[28] Swamikannu B, Umapathy VR, Natarajan PM, Nandini MS, Stylin AGSQ, Vimalarani V, Rajinikanth S. Unlocking the Therapeutic Benefits of Artemisia Annua: A Comprehensive Overview of its Medicinal Properties. Journal of Pharmacy and Bioallied Sciences. 2024; 16(5): S4248-S4253.
[29] Natarajan PM. Computational Studies on Recent Congeners of Fluoroquinolones and Nitroimidazoles for Their Use in Periodontal Therapy. Journal of Pharmacy and Bioallied Sciences. 2024; 16(5): S4731-S4740.
[30] Yadalam PK, Arumuganainar D, Natarajan PM, Ardila CM. Artificial intelligence-powered prediction of AIM-2 inflammasome sequences using transformers and graph attention networks in periodontal inflammation. Scientific Reports. 2025; 15: 8733.
[31] Yadalam PK, Chatterjee S, Natarajan PM, Ardila CM. Comparison of light gradient boosting and logistic r egression for interactomic hub genes in Porphyromonas gingivalis and Fusobacterium nucleatum-induced periodontitis with Alzheimer's disease. Frontiers in Oral Health. 2025; 6:1463458.
[32] Natarajan PM, Bhuminathan S, Leela B, Bindu K, Loganathan K, Ramachandran V. Smoking and its Role in Oral Cancer. Journal of Pharmacy and Bioallied Sciences 16(5): S4242-S4244.
[33] Yadalam PK, Natarajan PM, Ardila CM. Variational graph autoencoder for reconstructed transcriptomic data associated with NLRP3 mediated pyroptosis in periodontitis. Scientific Reports. 2025; 15: 1962.
[34] Daniel Raja FS, Abraham L, Rangasamy K, Saikia K, Rathankumar AK, Mironescu M, Mironescu I, Palanisamy CP, Kanniappan GV. Next-Generation Microbiome Therapeutics: Psychobiotics and Fecal Microbiota Transplants (FMT) for Mental Health Treatment. Frontiers in Cellular and Infection Microbiology. 2026; 16: 1719357.
[35] Dharmaprakash S, Gunasekaran VP, Sivaramakrishnan R, Kanniappan GV, Jayaraman S, Mironescu M, Rajabathar JR, Mironescu ID, Palanisamy CP. Marine macroalgae-mediated ultrasonic-assisted green synthesis of CuO nanoparticles embedded in starch/PVA electrospun nanoscaffolds for in vitro α-amylase and α-glucosidase inhibitory activity. Scientific Reports. 2026.
[36] Surendran N, Chandrasekaran G, Raju MV, Chandrasekaran MK, Ahalliya RM, Palanisamy CP, Kanniappan GV, Arcot R, Alharbi NS, Thiruvengadam M. Anti-inflammatory potential of ethanolic extract of Maranta arundinacea L.: Insights from COX-2 modulation and oxidative stress analysis. South African Journal of Botany. 2026; 195: 142-151.
[37] Pei J, Senthilkumar MV, Hessini K, Subramaniyam S, Sivaramakrishnan R, Kanniappan GV, Jayaraman S, Palanisamy CP. Green fabrication of starch/PVA/CuO nanoscaffolds using marine macroalgae extract for enhanced anti-inflammatory activity. Sustainable Chemistry and Pharmacy. 2026; 51: 102397.

[38] Balasubramanian V, Loganathan L, Muthuswamy K, Viswanathan TM, Raju MV, Chandrasekaran MK, Ahalliya RM, Poorasamy J, Palanisamy CP, Dominic S, Kanniappan GV. Anticancer therapeutic efficacy of PEGylated β-galactosidase from Aspergillus terreus in DMBA-induced breast cancer: Toxicological, molecular and histopathological evaluation in Wistar rats. International Journal of Biological Macromolecules. 2026; 360: 151856.
[39] Jayaraman S, Eswaran A, Rajagopal P, Palanisamy CP, Veerakumar P, Veeraraghavan VP, Sirasanagandla SR. Neuroendocrine-associated epigenetic factors in cellular senescence: mechanisms and therapeutic implications. Biogerontology. 2026; 27(2): 64.
[40] Ponnusamy B, Rajagopal P, Palanisamy CP, Veeraraghavan VP, Jayaraman S. Mechanistic Exploration of the anticancer activity of Justicia adhatoda Plant Leaf Ethanolic Extract against Colon Cancer Cells: An in silico and in vitro Approach. Asian Pacific Journal of Cancer Prevention. 2026; 27(3): 1069-1080.
[41] Pei J, Saran VS, Sivaramakrishnan R, Kanniappan GV, Pandurangan V, Jayaraman S, Dhayalan VK, Mironescu M, Mironescu ID, Palanisamy CP. Ultrasonic-assisted, Sargassum ilicifolium (brown marine macroalgae)-mediated biogenic synthesis of CuO nanoparticles incorporated in starch/PVA electrospun nanoscaffolds: In vitro safety and antioxidant efficacy assessment. Bioorganic Chemistry. 2026; 173: 109679.
[42] Natarajan PM, Umapathy VR, Murali A, Swamikannu B. (2022). Computational Simulations of Identified marine-derived Natural Bioactive Compounds As Potential Inhibitors of Oral Cancer. Future Science OA. 2022; 8(3).
[43] Natarajan PM, Umapathy VR. Role of transcriptomics in the study of oral cancer. Frontiers in Oral Health. 2025; 6:1524364.
[44] Vidhyarekha U, Natarajan PM, Bhuminathan S, Sabarinathan J, Suba R, Vijayalakshmi P. Role of artificial intelligence in Oral Cancer. Advances in Public Health. 2024. 2024: 3664408.
[45] Ganesan A, Kumar NG, Natarajan PM, Gauthaman J. Automated classification of elongated styloid processes using deep learning models-an artificial intelligence diagnostics. Frontiers in Oral Health. 2025; 5: 1424840.
[46] Umapathy VR, Natarajan PM, Swamikannu B. Regenerative Strategies in Dentistry: Harnessing Stem Cells, Biomaterials and Bioactive Materials for Tissue Repair. Biomolecules. 2025; 15: 546.
[47] Natarajan PM. Dental Bioinformnatics-Current Scope and Future perspectives. Research Journal of Pharmacy and Technology. 2022;15(5):2351-6.
[48] Ganesan A, Kumar NG, Natarajan PM. Solanum trilobatum leaf extract-derived silver nanoparticles downregulate the PI3K/AKT/mTOR signaling pathway and attenuate oral squamous cell carcinoma cell proliferation. Journal of Herbmed Pharmacology. 2024; 13(2): 300-307.
[49] Perumal MKK, Renuka RR, Subbiah SK, Natarajan PM. Artificial intelligence-driven clinical decision support systems for early detection and precision therapy in oral cancer: a mini review. Frontiers in Oral Health. 2025; 6: 1592428.
[50] Ramesh E, Ganesan A, Lakshmi KC, Natarajan PM. Artificial intelligence-based diagnosis of oral leukoplakia using deep convolutional neural networks Xception and MobileNet-v2. Frontiers in Oral Health. 2025; 6: 1414524.
[51] Ganesan A, Kumar NG, Natarajan PM. Anticancer activity of silver nanoparticles synthesized from aqueous leaf extract of Solanum trilobatum (Purple fruit pea eggplant) on human oral cancer cells. Journal of Herbmed Pharmacololgy. 2024; 13(2): 260-268.
[52] Natarajan PM, Swamikannu B, Sivaraman NM, Stylin AGSQ. Prevention of Oral Cancer: A Comprehensive Guide. Journal of Pharmacy and Bioallied Sciences. 2024; 16(5): S4239-S4241.
[53] Guo H, Liu Y, Wan T, Song D, Palanisamy CP, Geng J, Pei J, Özmen S, El-Aty AMA. Toward personalized cancer management: Role of precision nutrition–diet interventions. Journal of Functional Foods. 2024; 123: 106584.
[54] Natarajan SR, Krishnamoorthy R, Alshuniaber MA, Al-Anazi KM, Farah MA, Rajagopal P, Palanisamy CP, Veeraraghavan VP, Jayaraman S. Identification of FOXM1 as a novel protein biomarker and therapeutic target for colorectal cancer progression: Evidence from immune infiltration and bioinformatic analyses. International Journal of Biological Macromolecules. 282 (Part 4): 137201.
[55] Rajendran MS, Jayaraman S, Khan JM, Jasmine S, Prabhakaran RK, Raju MV, Chandrasekaran MK, Ahalliya RM, Kannappan P, Palanisamy CP, Kanniappan GV. Investigating the colon toxicity and carcinogenic role of monosodium glutamate compared with Dimethylhydrazine in male Wistar rats: Exploring the link to childhood colon cancer risk. Journal of King Saud University - Science. 2024; 36(11): 103507.
[56] Kumarasamy RV, Natarajan P, Umapathy VR, Roy JR, Rab SO, Saeed M, Panagal M, Mironescu M, Srinivasan GP, Palanisamy CP. Clinical Applications and Therapeutic Potentials of Advanced Nanoparticles: A Comprehensive Review on Completed Human Clinical Trials. Frontiers in Nanotechnology. 2024; 6:1479993.
[57] Jin W, Pei JJ, Roy JR, Jayaraman S, Ahalliya RM, Kanniappan GV, Mironescu M, Palanisamy CP. Comprehensive review on single-cell RNA sequencing: A new frontier in Alzheimer's disease research. Ageing Research Reviews. 2024; 274: 102454.

[58] Pei J, Palanisamy CP, Jayaraman S, Natarajan PM, Umapathy VR, Roy JR, Panagal M, Jayaraman S. Curcumin-loaded polymeric nanomaterials as a novel therapeutic strategy for Alzheimer's disease: A comprehensive review. Ageing Research Reviews. 2024; 99: 102393.
[59] Pei J, Palanisamy CP, Jayaraman S, Natarajan PM, Umapathy VR, Roy JR, Thalamati D, Ahalliya RM, Kanniappan GV, Mironescu M. A comprehensive review on starch-based Sustainable Edible Films Loaded with Bioactive Components for Food Packaging. International Journal of Biological macromolecules. 2024; 274 (Part-1): 133332.
[60] Palanisamy CP, poompradub S, Sansanaphongpricha K, Subramani K, Sonsudin F. Increased expression levels of PDGF and VEGF magnify the wound healing potential facilitated by biogenic synthesis of silver nanoparticles. Nano-Structures & Nano-Objects. 2024; 39: 101236.
[61] Pei J, Palanisamy CP, Jayaraman S, Natarajan PM, Umapathy VR, Roy JR, Thalamati D, Ahalliya RM, Kanniappan GV, Mironescu M. Proteomics Profiling of Extracellular Vesicle for Identification of Potential Biomarkers in Alzheimer's Disease: A Comprehensive Review. Ageing Research Reviews. 2024; 99: 102359.
[62] Xi J, Wang T, Xian P, Liu X, Du M, Yang H, Palanisamy CP, Lin W, Long Q. Proteomic insights uncover enhanced neurotherapeutic potential in conditioned mesenchymal stem cell-derived extracellular vesicles. Extracellular Vesicle. 2024; 3: 100037.
[63] Pei J, Natarajan PM, Umapathy VR, Swamikannu B, Sivaraman NM, Krishnasamy L, Palanisamy CP. Advancements in the synthesis and functionalization of zinc oxide-based nanomaterials for enhanced oral cancer therapy. Molecules. 2024; 29(11): 2706.
[64] Gatasheh MK, Natarajan SR, Krishnamoorthy R, Alsulami TS, Rajagopal P, Palanisamy CP, Veeraraghavan VP, Jayaraman S. Molecular analysis to identify novel potential biomarkers as drug targets in colorectal cancer therapy: an integrated bioinformatics analysis. Molecular and Cellular Oncology. 2024; 11(1): 2326699.
[65] Pei J, Yan Y, Jayaraman S, Rajagopal P, Natarajan PM, Umapathy VR, Gopathy S, Roy JR, Sadagopan CS, Thalamati D, Palanisamy CP, Mironescu M. A review on advancements in the application of starch-based nanomaterials in biomedicine: Precision drug delivery and cancer therapy. International Journal of Biological Macromolecules. 2024; 130746.
[66] Pei JJ, Yan Y, Palanisamy CP, Jayaraman S, Natarajan PM, Umapathy VR, Gopathy S, Roy JR, Sadagopan JC, Thalamati D, Mironescu M. Materials-based drug delivery approaches: Recent advances and future perspectives. Green Processing and Synthesis. 2024; 13: 20230094.
[67] Pei JJ, Deng W, Liu Y, Guo Y, Chen J, Abdu H, Khan MR, Palanisamy CP, El-Aty AM. A Comprehensive Review of Cornus officinalis: Health Benefits, Phytochemistry, and Pharmacological Effects for Functional Drug and Food Development. Frontiers in Nutrition. 2023; 10: 1309963.
[68] Alugoju P, Palanisamy CP, Anthikapalli NVA, Jayaraman S, Prasanskulab A, Chuchawankul S, Dyavaiah M, Tencomnao T. Exploring the anti-aging potential of natural products and plant extracts in budding yeast Saccharomyces cerevisiae: A review. F1000Research. 2023; 12: 1265.
[69] Lavanya M, Krishnamoorthy R, Alshuniaber MA, Manoharadas S, Palanisamy CP, Veeraraghavan VP, Jayaraman S, Rajagopal P, Padmini R. Formulation, characterization and evaluation of gelatin-syringic acid/zinc oxide nanocomposite for its effective anticancer, antioxidant and anti-inflammatory activities. Journal of King Saud University-Science. 2023; 35: 102909.
[70] Palanisamy CP, Poompradub S, Sansanaphongpricha K, Jayaraman S, Subramani K, Sonsudin F. Biosynthesis of silver nanoparticles (AgNPs) using ethanolic extract of Nigella sativa (L.) seeds promotes wound healing via PDGF and VEGF signalling pathways activation. Biocatalysis and Agricultural Biotechnology. 2023; 54: 102970.
[71] Prasad M, Jayaraman S, Natarajan SR, Veeraraghavan VP, Krishnamoorthy R, Gatasheh MK, Palanisamy CP, Elrobh M. Piperine modulates IR/Akt/GLUT4 pathways to mitigate insulin resistance: Evidence from animal and computational studies. International Journal of Biological Macromolecules. 2023; 253: 127242.
[72] Palanisamy CP, Pei JJ, Phaniendra A, Venkata AAN, Jayaraman S, Veeraragahavan VP, Sridevi G, Roy JR, Janaki CS, Thalamati D, Mironescu M, Luo Q, Chai Y, Long Q. New Strategy of Neurodegenerative Disease Treatment with Extracellular Vesicles (EVs) Derived from Mesenchymal Stem Cells (MSCs). *Theranostics*. 2023; 13(12):4138-4165. doi:10.7150/thno.83066.
[73] Palanisamy CP, Phaniendra A, Jayaraman S, Poompradub S. *Nigella sativa* L. seed extracts promotes wound healing progress by activating VEGF and PDGF signalling pathways: *An in vitro* and *in silico* study. *F1000 Research*. 2023; 12: 436.
[74] Pei JJ, Palanisamy CP, Phaniendra A, Venkata AAN, Natarajan PM, Umapathy VR, Swamikannu B, Jayaraman S, Rajagopal P, Poompradub S. A comprehensive review on bio-based materials for chronic diabetic wounds. *Molecules*. 2022; 28(2), 604.